

Bidentate Urea Derivatives of *p*-*tert*-Butyldihomooxalix[4]arene: Neutral Receptors for Anion Complexation

Paula M. Marcos,^{*,†,‡} Filipa A. Teixeira,[†] Manuel A. P. Segurado,^{†,‡} José R. Ascenso,[§] Raul J. Bernardino,^{||} Sylvia Michel,^{⊥,#} and Véronique Hubscher-Bruder^{⊥,#}

[†]Centro de Ciências Moleculares e Materiais, Faculdade de Ciências da Universidade de Lisboa, Edifício C8, 1749-016 Lisboa, Portugal

[‡]Faculdade de Farmácia da Universidade de Lisboa, Av. Prof. Gama Pinto, 1649-003 Lisboa, Portugal

[§]Instituto Superior Técnico, Complexo I, Av. Rovisco Pais, 1049-001 Lisboa, Portugal

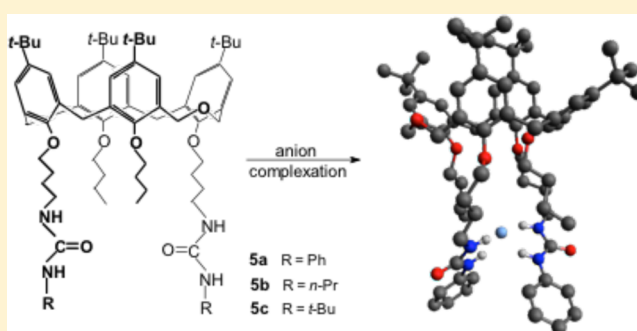
^{||}Laboratory of Separation and Reaction Engineering, ESTM, Instituto Politécnico de Leiria, Santuário Na. Sra. dos Remédios, Apartado 126, 2524-909 Peniche, Portugal

[⊥]Université de Strasbourg, IPHC, 25 rue Becquerel 67087 Strasbourg, France

[#]CNRS, UMR7178, 67037 Strasbourg, France

Supporting Information

ABSTRACT: Three new bidentate ureidodihomooxalix[4]-arene derivatives (phenyl **5a**, *n*-propyl **5b**, and *tert*-butyl **5c**) were synthesized in four steps from the parent compound *p*-*tert*-butyldihomooxalix[4]arene and obtained in the cone conformation, as shown by NMR studies. The binding ability of these neutral receptors toward spherical, linear, trigonal planar, and tetrahedral anions was assessed by ¹H NMR and UV–vis titrations. The structures and complexation energies of some complexes were also studied by DFT methods. The data showed that the association constants are strongly dependent on the nature of the substituent (aryl/alkyl) at the urea moiety. In general, for all the receptors, the association constants decrease with decrease of anion basicity. Ph-urea **5a** is the best anion receptor, showing the strongest complexation for F[−] (log *K*_{assoc} = 3.10 in CDCl₃) and also high binding affinity for the carboxylates AcO[−] and BzO[−]. Similar results were obtained by UV–vis studies and were also corroborated by DFT calculations.



INTRODUCTION

Calixarene-based molecules, in particular lower rim derivatives, have been widely used in the last three decades as metal cation binders.^{1a–c} Conversely, the binding of anions by these macrocycles has received less attention in the past. Selective complexation of anions is more demanding than that of cations, mainly because of some unique properties of anions that need to be taken into account in the design of the receptors. Compared to cations, anions are larger and therefore have a lower charge to radius ratio. Consequently, they show less effective electrostatic interactions. They present a wide range of geometries and pH dependence, and they are more affected by solvation. However, more recently, the study of anion receptors based on calixarenes, as well as on other macrocycle compounds, has gained a growing interest due to the important role displayed by anions in biology, medicine, and environmental areas.^{2–6}

To add hydrogen bond donor groups to organic hosts has been an important task for obtaining recognition for specific anions. Thus, urea and thiourea binding groups have been widely incorporated in the calixarene scaffold to produce anion

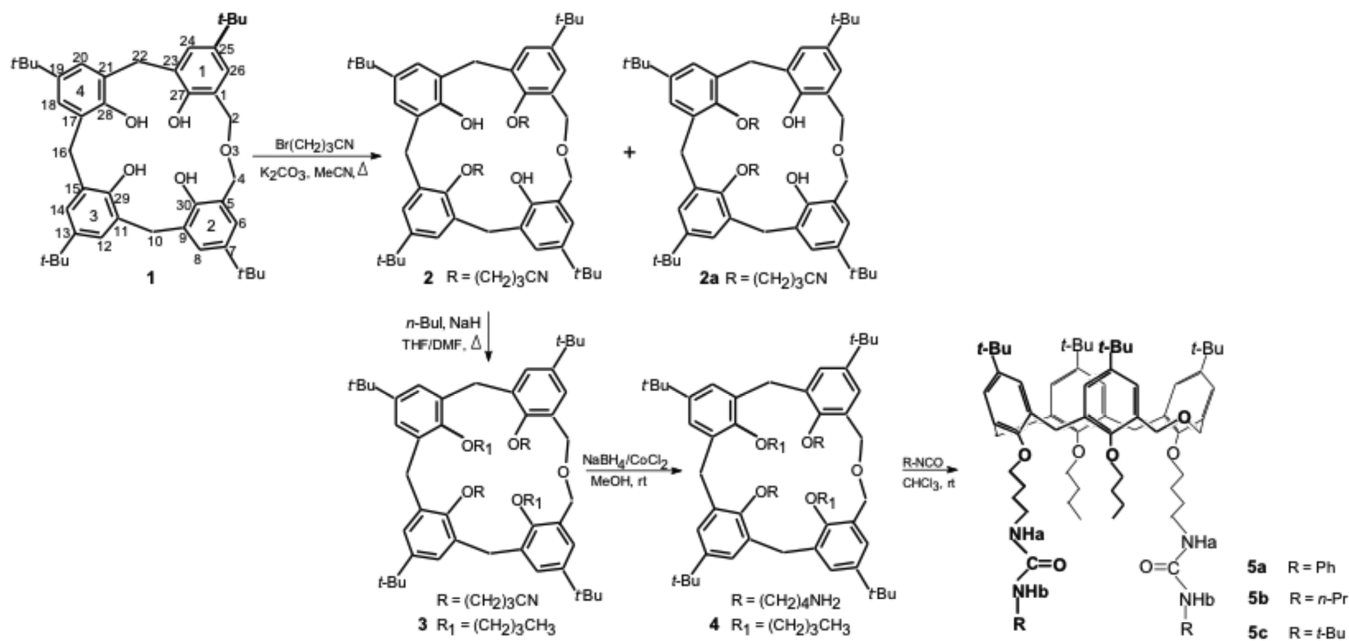
receptors. These groups provide effective and directional hydrogen bonds. Over the last 15 years, calix[4]arene scaffolds, incorporating one or more urea and thiourea moieties at the lower^{7–11} or upper rim,^{12–14} have been the most studied for anion recognition. Ureidocalix[5]arene¹⁵ and calix[6]arene^{16,17} derivatives have also been tested as anion receptors.

Following our previous studies on the cation binding properties of dihomooxalix[4]arenes (calix[4]arene analogues in which one CH₂ bridge is replaced by one CH₂OCH₂ group),¹⁸ we have recently extended our research into the study of anion complexation. Dihomooxalix[4]arenes have cavity sizes slightly larger than those of calix[4]arenes; they are therefore more flexible, but possess a cone conformation, being potential hosts for larger anions. This paper reports the synthesis, the NMR conformational analysis, and the complexation properties of three new bidentate urea derivatives of *p*-*tert*-butyldihomooxalix[4]arene toward a large variety of anions (spherical, linear, trigonal planar, and tetrahedral).

Received: November 27, 2013

Published: December 23, 2013

Scheme 1. Synthetic Route for the Preparation of Bidentate Urea Derivatives 5a–c



These properties have been assessed by proton NMR and UV absorption spectrophotometric studies. The structures and complexation energies for some urea-anion systems were also investigated by theoretical studies using DFT methods. The results are compared to those obtained with closely related calix[4]arene derivatives and discussed in terms of the nature of the substituent (aryl/alkyl) at the urea moiety.

RESULTS AND DISCUSSION

Synthesis and NMR Conformational Analysis. Following our recent interest in anion binding by homooxalixarenes modified with substituted urea groups at the lower rim, and to overcome the difficulties found to obtain the tetra-[(cyanopropyl)oxy] derivatives (precursors to urea-terminated compounds) in the cone conformation,¹⁹ we decided to try the synthesis of bidentate urea derivatives. Thus, the parent compound *p*-*tert*-butyldihomooxalix[4]arene (**1**) was treated with 2 equiv of 4-bromobutyronitrile and K_2CO_3 in refluxing acetonitrile for 6 days (Scheme 1). This reaction afforded a mixture composed of two disubstituted compounds. Separation by flash chromatography gave the 1,3-dicyanodihydroxy derivative **2** as the main product, along with a small amount of the 3,4-dicyanodihydroxy derivative **2a**.

The ^1H NMR spectrum of **2** displays four singlets for the *tert*-butyl groups, five AB quartets for the CH_2 bridge protons, four pairs of doublets for the aromatic protons, two singlets for the OH groups, and several multiplets for the $-\text{OCH}_2\text{CH}_2\text{CH}_2\text{CN}$ methylene protons. The ^{13}C NMR spectrum shows three ArCH_2Ar resonances at 29.3, 30.0, and 32.7 ppm, indicating a cone conformation for this derivative.²⁰ Compound **2a** exhibits symmetric NMR spectra. The ^1H NMR spectrum shows two singlets for the *tert*-butyl groups, three AB quartets in a 2:2:1 ratio for the CH_2 bridge protons, five multiplets for the $-\text{OCH}_2\text{CH}_2\text{CH}_2\text{CN}$ groups, two pairs of doublets for the aromatic protons, and one singlet for the OH groups. The ^{13}C NMR spectrum displays two ArCH_2Ar resonances at δ 30.7 (one carbon atom) and δ 31.6 (two carbon atoms), indicating a cone conformation. For both

compounds, the cone conformation and the substitution patterns were further confirmed by proton–proton correlations observed in the NOESY spectra. As previously described by us for the formation of other disubstituted dihomooxalix[4]-arenes,²¹ the preferential formation of the 1,3-disubstituted derivative is expected. This type of substitution (Scheme 1) was confirmed for the asymmetric compound **2** (Figure 1) through

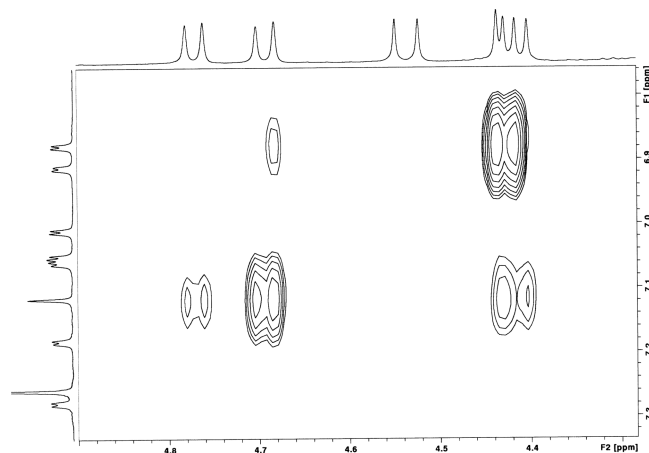
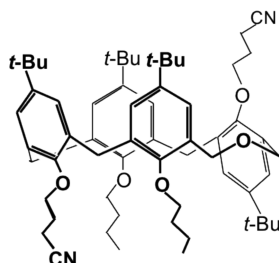


Figure 1. Section of the NOESY spectrum of 1,3-dicyanodihydroxy derivative **2**.

the simultaneous observation of two NOE effects between the OH proton at 7.12 ppm (position 30) and two axial methylene protons at 4.42 and 4.69 ppm (positions 10 and 4, respectively). In the case of the symmetric compound **2a** (Figure S1, Supporting Information), the 3,4-disubstituted pattern (Scheme 1) was confirmed by two simultaneous NOE effects observed between the OH proton (position 27) and two axial methylene protons at 4.20 and 4.67 ppm (positions 22 and 2, respectively), as well as between the (cyanopropyl)oxy protons (position 28) and the two axial methylene protons at 4.20 and 4.45 ppm (positions 22 and 16, respectively).

Derivative **2** was further alkylated with *n*-butyl iodide and NaH in THF/DMF, yielding dicyanodibutoxy derivative **3** in the cone (major product) and partial cone A (Scheme 2)

Scheme 2. Dicyanodibutoxy Derivative **3** in the Partial Cone A Conformation



conformations. After separation of the two conformers, the ^{13}C NMR spectra displayed three ArCH_2Ar resonances around 30 ppm for the cone conformer and three ArCH_2Ar resonances, one around 39 ppm and the other two at 30 ppm, for the partial cone A conformer.²² The ^1H NMR spectrum of the latter conformer displays an upfield multiplet (δ 0.73 ppm) corresponding to four methylene protons of an inverted group.¹⁹ According to the COSY spectrum, these protons have no correlations with the methyl protons at 0.96 ppm, which indicates that they belong to a (cyanopropyl)oxy group and not to a (butyl)oxy group. Moreover, the identification of the inverted group was further corroborated by proton–proton correlations observed in a NOESY spectrum, mainly by the NOE enhancement observed between the aromatic proton at

7.03 ppm (position 20) and those methylene protons at 0.73 ppm (Figure S2, Supporting Information).

Reduction of the cyano groups of the cone derivative **3** with borohydride and cobalt chloride in methanol gave the diamine **4**, which reacted with aryl or alkyl isocyanate in chloroform to give the corresponding diaryl or dialkylurea derivatives (phenyl **5a**, *n*-propyl **5b**, and *tert*-butyl **5c**) in the cone conformation. These compounds have no symmetry. They are inherently chiral, as indicated by their NMR spectra. All the ureido derivatives show clear and sharp proton NMR spectra in CDCl_3 at room temperature and independent of the concentration, indicating absence of self-aggregation.^{13,14} Parts a–c of Figure 2 show a section of those spectra with the two NHa and the two NHb protons of the ureido groups at the expected chemical shifts. When a more polar solvent like DMF was used, the NH signals remained sharp but shifted downfield, in agreement with the formation of intermolecular hydrogen bonds between the ureido groups and the solvent (see, for example, *n*-Pr-urea **5b**, Figure 2d).

Anion-Binding Studies. ^1H NMR Studies. The binding affinity of bidentate ureas **5a**, **5b**, and **5c** toward anions of spherical (F^- , Cl^- , Br^- , I^-), trigonal planar (NO_3^- , AcO^- , BzO^-), linear (CN^- , SCN^-), and tetrahedral (HSO_4^- , H_2PO_4^- , ClO_4^-) geometries was investigated in CDCl_3 by ^1H NMR titrations using tetrabutylammonium salts. The association constants, reported in Table 1, were determined following the urea NH chemical shift and using the WinEQNMR2 program.²³ In a few cases where those protons became broad or even completely disappeared, the binding constants were determined from the complexation induced shifts of the aromatic protons of the calixarene framework. The titration

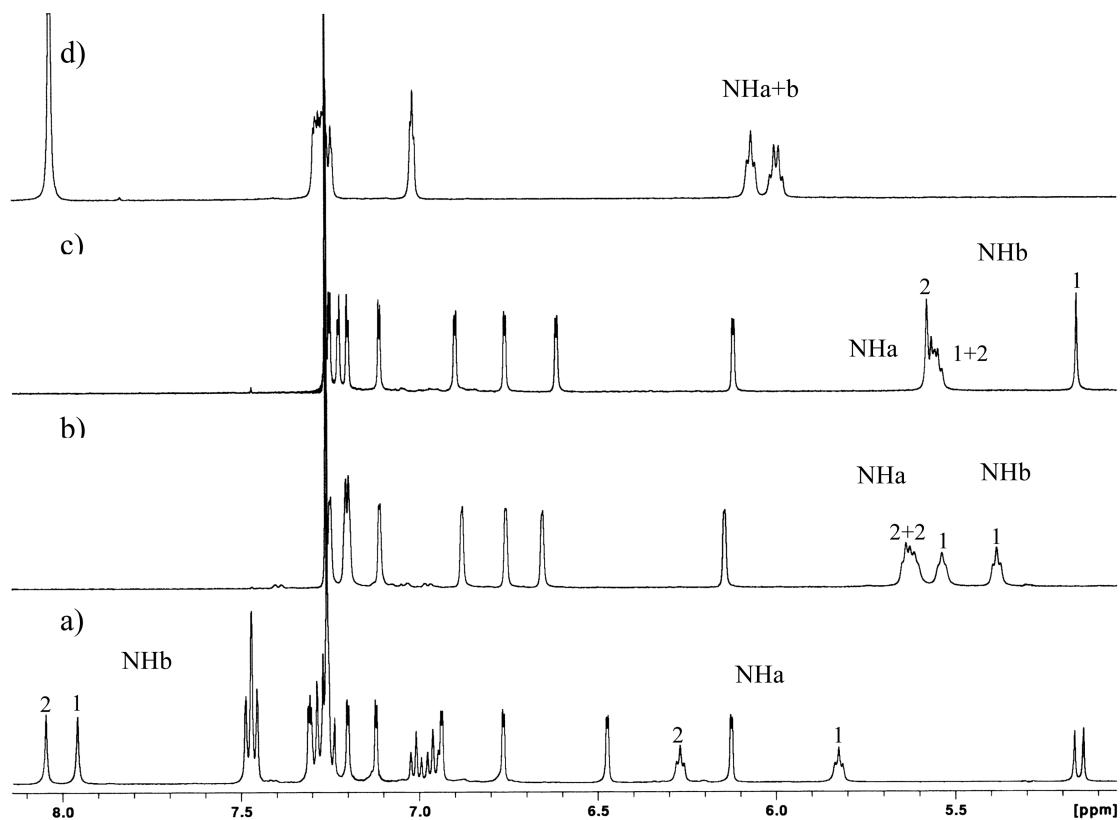


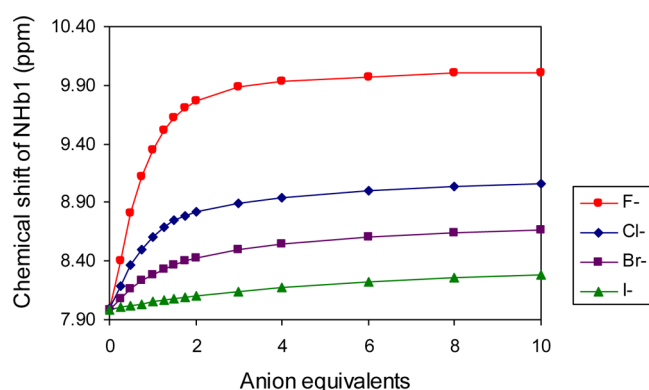
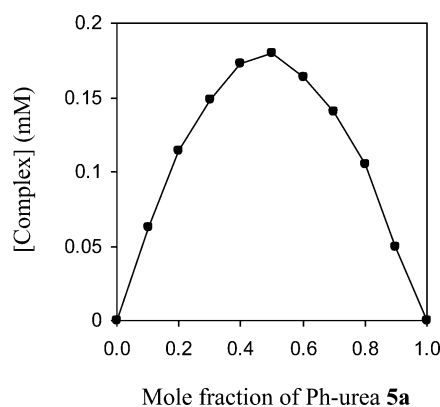
Figure 2. Partial ^1H NMR spectra (500 MHz, CDCl_3 , 22 °C) of (a) Ph-urea-**5a**, (b) *n*-Pr-urea **5b**, (c) *t*-Bu-urea **5c**, (d) *n*-Pr-urea **5b** in $\text{DMF-}d_7$.

Table 1. Association Constants ($\log K_{\text{assoc}}$)^a of Dihomooxa Bidentate Ureas **5a–c** in CDCl_3 at 25 °C Determined by ¹H NMR Experiments

	spherical				linear		trigonal planar			tetrahedral		
	F [−]	Cl [−]	Br [−]	I [−]	CN [−]	SCN [−]	NO ₃ [−]	AcO [−]	BzO [−]	HSO ₄ [−]	H ₂ PO ₄ [−]	ClO ₄ [−]
i. radius ^b (Å)	1.33	1.81	1.96	2.20	1.91	2.13	1.79	2.32		1.90	2.00	2.40
Ph-urea 5a	3.10	2.73	2.23	1.59	2.71	1.90	2.42	2.88	2.93	2.58	2.69	1.65
<i>n</i> -Pr-urea 5b	1.65	1.57	1.35	1.34	1.61	1.46	1.54	1.59	1.65	1.40	1.21	1.56
<i>t</i> -Bu-urea 5c	1.38	1.21	1.02	1.18	1.28	1.20	1.00	0.90	0.89	1.05	1.17	1.13

^aEstimated error <10%. ^bData quoted in Marcus, I. *Ion Properties*; Marcel Dekker: New York, 1997; pp 50–51.

profiles obtained in all cases (see for example Figure 3) clearly indicate the formation of 1:1 receptor–anion complexes, being this stoichiometry also confirmed by Job plots (see as an example the Job curve for **5a** + Br[−], Figure 4).

**Figure 3.** Titration curves of Ph-urea **5a** with TBA salts in CDCl_3 .**Figure 4.** Job plot based on ¹H NMR data for Ph-urea **5a** + Br[−]; total concentration 5×10^{-3} M in CDCl_3 .

The data show that the association constants for anion binding with the receptors **5a**, **5b**, and **5c** strongly depend on the nature of the substituted (aryl/alkyl) at the urea moiety. In general, arylureas are stronger anion receptors than alkylureas because of the higher acidity of their ureido NHs.³ Ph-urea derivative **5a** is the best anion receptor, displaying moderate to reasonably high binding ability. *n*-Pr-urea **5b** and *t*-Bu-urea **5c** are weak receptors, with **5b** being slightly better than **5c**. The higher flexibility and the less bulky shape of the R group in the former receptor may lead to a conformational arrangement more favorable to the NH hydrogen bond donation. However, the three receptors show the same trend in the anion-binding affinities. The addition of anions to the receptors (**5a–c**) caused more or less significant downfield shifts of the NH

protons, clearly indicating hydrogen-bonding interactions. In all cases, a fast exchange rate between the complexed and the free host was observed on the NMR time scale at room temperature. With very few exceptions, the association constants of **5a–c** with the anions decrease in the order of the anion basicity in CHCl_3 (Table 2). Although no $\text{p}K_{\text{a}}$ values

Table 2. Anion Basicity in CHCl_3 and MeCN

geometry	anion basicity ($\text{CHCl}_3/\text{MeCN}$)
spherical	F [−] > Cl [−] > Br [−] > I [−]
linear	CN [−] > SCN [−]
trigonal planar	AcO [−] > BzO [−] > NO ₃ [−]
tetrahedral	H ₂ PO ₄ [−] > HSO ₄ [−] > ClO ₄ [−]

were found in this solvent, it is known that $\text{p}K_{\text{a}}$ values follow the same trends in similar solvents.²⁴ Thus, it is completely justifiable to assume the same $\text{p}K_{\text{a}}$ order in CHCl_3 as was reported in 1,2-dichloroethane.

A systematic observation of the data in Table 1 and Figure 3 reveals that in the case of the halogen anions (spherical geometry) the addition of 2 equiv of TBA iodide to Ph-urea **5a** causes a small downfield shift for the urea NHb₁ proton (0.12 ppm), which increases for Br[−] (0.44 ppm) and even more for Cl[−] (0.83 ppm). In the case of F[−] a large downfield shift of 1.82 ppm can be observed, as well as another of 1.52 ppm for NHa₁ proton. Small downfield shifts for the *ortho* protons and small upfield shifts for the *meta* and *para* protons of the phenyl urea groups are also observed, as mentioned before for other analogue receptors,^{7,10,25} and corroborate the expected effects for the formation of hydrogen-bonding complexes. These effects are the result of both the increase of electron density on the phenyl rings (through-bond) causing a shielding effect, and the polarization of the C–H bonds (through-space) causing a deshielding effect.⁵ **5a** displays a $\log K_{\text{assoc}}$ of 3.10 for F[−], the highest value obtained with these dihomooxa urea receptors. It shows some selectivity over Cl[−] and Br[−] ($S_{\text{F}^-}/X^- = 2.3$ and 7.4, respectively). The same trend is observed for urea derivatives **5b** and **5c** (K_{assoc} decreases with decreasing of anion basicity), except for *t*-Bu-urea **5c** with I[−], which displays a slightly higher K_{assoc} than that with Br[−].

Our results with F[−] showed no evidence for the formation of the HF₂[−] species, either generated in situ due to trace amounts of water²⁶ or by deprotonation of the receptor.^{10,27,28} Thus, no sigmoidal shape can be observed in the titration curve shown in Figure 3, and the chemical shifts of the relevant protons followed the expected variations for the formation of an H-bond complex, namely the *ortho* protons of the urea phenyl rings, as mentioned before. These protons experienced small downfield shifts during all the titration ($\Delta\delta = 0.10$ ppm with 10 equiv of F[−]). On the other hand, the acidity of Ph-urea **5a** is lower when compared to receptors containing electron-

withdrawing groups, such as NO_2 .²⁸ In addition, solvent polarity plays an important role in stabilizing the H-bond complexes. The higher the polarity of the solvent ($\text{DMSO} > \text{MeCN} > \text{CHCl}_3$), the lower the stability of the H-bond complex. It was reported that in the poorly polar CH_2Cl_2 , the 1,3-bis(4-nitrophenyl)urea gave only the H-bond complex with F^- .²⁸ In addition, deprotonation was never reported in CHCl_3 .²⁵

In the presence of the pseudohalides CN^- and SCN^- (linear geometry) a similar behavior was observed for all the receptors, which followed the same trend observed for the halogens. The more basic anion CN^- was better complexed, mainly with Ph-urea **5a**, that exhibited a $\log K_{\text{assoc}}$ of 2.71 and selectivity over SCN^- of 6.5.

Concerning the trigonal planar oxoanions, Ph-urea **5a** showed a high binding affinity toward the carboxylates BzO^- and AcO^- ($\log K_{\text{assoc}}$ of 2.93 and 2.88, respectively). In contrast to the previous situations, the trend observed with these oxoanions was slightly different. Receptors **5a** and **5b** displayed association constants that slightly increased from AcO^- to BzO^- and then decreased from BzO^- to NO_3^- (as expected). This slight inversion of the expected order for AcO^- and BzO^- according to their basicities is within the experimental error, and has no meaning if we compare the differences between the $\text{p}K_{\text{a}}$ of the corresponding acids in CHCl_3 [$\Delta\text{p}K_{\text{a}}$ ($\text{AcOH} \rightarrow \text{BzOH}$) = 1.7 and $\Delta\text{p}K_{\text{a}}$ ($\text{BzOH} \rightarrow \text{HNO}_3$) = 12.6].²⁹ This means that AcO^- is a base only 50 times stronger than BzO^- , while NO_3^- is a base almost 4×10^{12} times weaker than BzO^- ! However, as that inversion was not maintained in the UV studies (discussed below), a possible explanation may lie in a specific solvation mode of the urea–benzoate complexes in chloroform. *t*-Bu-urea **5c** is the weakest receptor, displaying a slightly higher $\log K_{\text{assoc}}$ value for the smaller anion NO_3^- . This may be due to steric hindrance caused by the *t*-Bu groups.

Finally, concerning the tetrahedral oxoanions, Ph-urea **5a** followed the anion basicity order and exhibited much higher binding affinities toward H_2PO_4^- and HSO_4^- than to ClO_4^- . In the case of *n*-Pr-urea **5b** the basicity order is inverted. The less basic and largest anion ClO_4^- is slightly better complexed than the others. This may be due to a suitable size complementarity of **5b** and the anion. Size-dependent binding has already been described, mainly for the spherical halides.¹² Furthermore, *n*-Pr-urea should have enough flexibility to allow a good binding environment in terms of size matching. *t*-Bu-urea **5c** showed again the lowest $\log K_{\text{assoc}}$ values, but following the basicity order.

UV–vis Studies. The interactions between Ph-urea **5a** and some anions of different geometries (F^- , Cl^- , SCN^- , NO_3^- , AcO^- , BzO^- , HSO_4^- , and H_2PO_4^-) as TBA salts have also been studied by UV–vis absorption spectrophotometry in MeCN.

Significant spectral changes were observed for **5a** in the presence of F^- , AcO^- , BzO^- , and H_2PO_4^- , as shown in Figure 5 for AcO^- as an example. Very small or no spectral changes occurred for all other systems, which could not be interpreted. As revealed by the association constant data (Table 3), Ph-urea **5a** displayed the strongest complexation for F^- ($\log K_{\text{assoc}} = 4.6$), closely followed by AcO^- , BzO^- , and H_2PO_4^- in agreement with the basicity order in MeCN. Compound **5a** forms 1:1 and also 2:1 complexes with all the anions and presents higher association constants than by NMR. It should be noted that in UV titration experiments the concentrations are much lower than those used in NMR, and this difference

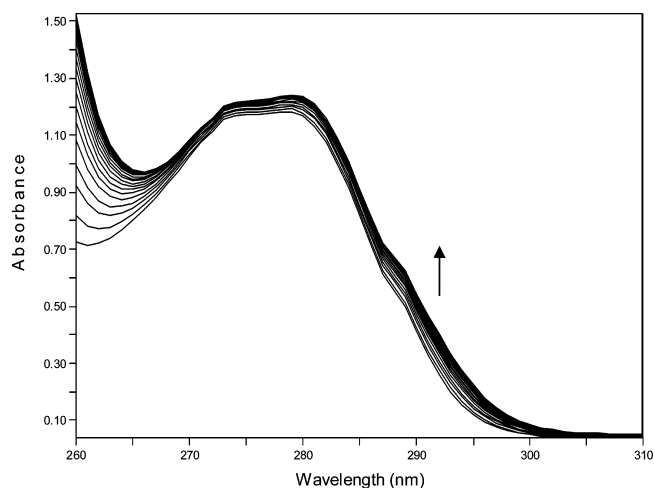


Figure 5. Changes in the UV spectra of **5a** upon addition of acetate ($C_L = 1.95 \times 10^{-4}$ M; $0 \leq R = C_A/C_L \leq 2$) in MeCN. The arrow indicates the increasing amounts of acetate.

Table 3. Association Constants ($\log K_{\text{assoc}}$)^a of Ph-urea **5a** in MeCN at 25 °C Determined by UV–vis Experiments

	X:L	F^-	AcO^-	BzO^-	H_2PO_4^-
Ph-urea 5a	1:1	4.6	4.5	4.2	4.2
	2:1	4.6	4.3	4.4	4.0

^aValues are the average of at least two experiments; estimated error <10%.

can influence the stoichiometry of the species formed and also their association constants. The more diluted solutions used in UV studies favor the dissociation of the salts, providing a higher concentration of the anions available for complexation, and consequently the association constants become higher. Similar situations were reported before with other receptors.^{14,15,25} However, these UV results follow the same trend observed in the NMR studies discussed above. No positive cooperative effect is observed, as the association constants are lower for the second complexation step than for the 1:1 complexes (except in the case of BzO^-).

DFT Studies. The binding affinity of Ph-urea **5a** was also studied by DFT methods to give more insight into the structures and electronic properties of the complexes.

All the structures (receptor and complexes) were fully optimized without symmetry constraints using the Becke three-parameter hybrid functional combined with the Lee, Yang, and Parr correlation functional (B3LYP).³⁰ Although the comparison between gas-phase and condensed-phase structures is not direct, all the structures were geometry optimized solvent free. They are therefore expected to correlate primarily with gas state complex geometries and not necessarily with NMR data, in which the solvent will influence the anion–receptor interactions and the relative complexation energies. However, they can give some insight into the key differences between the complexes under investigation.

The interactions of **5a** with some anions of each geometry group (F^- , Cl^- , SCN^- , CN^- , AcO^- , BzO^- , HSO_4^- , and H_2PO_4^-) were studied, and their minimum energy structures were initially determined with the B3LYP/3-21G basis set. After this minimization, single-point energy calculations were then carried out at the B3LYP/6-31G(d,p) level, to add polarization functions for hydrogen atoms and diffuse functions

for both hydrogen and non-hydrogen atoms, to obtain a more accurate description of the hydrogen-bonding interactions involved in the complexation of the anions.³¹

The energies obtained for all the anion–receptor 1:1 complexes, either by optimization or single point, are presented in Table 4. All of the complexation energies calculated were

Table 4. Total Energies E (au) and Complexation Energies ΔE_c (kcal mol⁻¹)^a for the Systems Studied. Optimization at B3LYP/3-21G and Single-Point at B3LYP/6-31G(d,p) Levels

	B3LYP/3-21G		B3LYP/6-31G(d,p)	
	E	ΔE_c^a	E	ΔE_c^a
5a	-3645.10924		-3665.19423	
5a·F ⁻	-3744.53902	-175.30	-3765.14991	-126.50
5a·Cl ⁻	-4103.25415	-55.11	-4125.53025	-52.57
5a·AcO ⁻	-3872.46085	-86.72	-3893.79082	-62.56
5a·BzO ⁻	-4063.14083	-67.23	-4085.53032	-49.03
5a·HSO ₄ ⁻	-4341.12293	-69.84	-4364.91281	-41.14
5a·H ₂ PO ₄ ⁻	-4285.30927	-71.69	-4308.83746	-45.95
5a·CN ⁻	-3737.51271	-69.88	-3758.11448	-60.07
5a·SCN ⁻	-4133.79539	-40.39	-4156.35055	-35.75

^a ΔE_c corresponds to the process $5a + X^- \rightarrow [5a \cdot X^-]$, where X^- represents each one of the anions.

negative, meaning that the complexes were thermodynamically favorable. The relative complexation energies were, however, very different. In general, it can be observed that independently of the basis set used (3-21G or 6-31G(d,p)), the stability of the complexes decrease with decreasing of anion basicity. The most stable complex was obtained with F⁻ with a complexation energy double of the following one (5a·AcO⁻). Moreover, the difference in energy between the two spherical anions F⁻ and Cl⁻ is much higher than the difference in energy between the two trigonal planar oxoanions AcO⁻ and BzO⁻ ($\Delta E_c = 73.93$ and 13.53 kcal mol⁻¹, respectively). This is in complete agreement with the strength of these bases in CHCl₃ [ΔpK_a (HF \rightarrow HCl) = 15.5 and ΔpK_a (AcOH \rightarrow BzOH) = 1.7].²⁹

Figure 6 shows the optimized structures for Ph-urea 5a and the eight complexes studied. It can be observed that the free receptor presents a distorted cone conformation, which becomes more symmetric upon the anion complexation, being this more noticeable in the case of F⁻. It is also clear from Figure 6 (b and c) that for the spherical F⁻ and Cl⁻ a cage structure was formed with all four NH ureido groups directed into the center of the cavity, in which the anion is included. In the case of the linear CN⁻ and SCN⁻ anions (Figure 6, h and i), the four hydrogen bonds are directed into the more electronegative atom, while for the oxoanions they are directed to both oxygen atoms (or to the three oxygens in the case of HSO₄⁻) of the anion molecule. This is confirmed in Table 5, where hydrogen-bond distances are listed. As expected, all the anions interact preferably with the four hydrogen atoms of the NH ureido groups. According to the distances NH...X⁻ shown in Table 5, it is evident a strong concordance between these distances and the stability of the complexes, namely for F⁻ and AcO⁻ that show the shortest distances (in average 1.69 and 1.81 Å, respectively).

To better characterize and visualize the electrostatic equilibria in the complexes, electrostatic potential maps were calculated over an electronic isodensity surface of $\rho = 0.05$ Å⁻³ (Figure 7). Red regions are those of relatively lower or more

negative electrostatic potential, while the blue ones correspond to higher or more positive electrostatic potential. Three structures are presented here: the receptor, the most stable complex (5a·F⁻), and the least stable complex (5a·SCN⁻). In all of the structures the oxomethylene bridge is a zone with negative electrostatic potential as well as the oxygen atom of the urea fragment. The presence of the anion pulls the lower limit of the electrostatic potential further down when compared to the free receptor. Also visible are the hydrogen bonds between the more electronegative atoms of the anions and the hydrogens of the NH ureido moiety. Overall, these structural representations give insights to the electrostatic rearrangement caused by the introduction of the anion molecules. Although the electrostatic potentials of the complexes are similar (Figure 7, b and c), the potential energy associated with each anion is very different, as represented by the color distribution observed.

CONCLUSIONS

A new family of anion receptors based on dihomooxalix[4]-arenes containing two urea moieties at the lower rim via a four carbon atom spacer, has been described. Three bidentate ureido derivatives (phenyl 5a, *n*-propyl 5b, and *tert*-butyl 5c) were obtained in the cone conformation and complexed anions in a 1:1 stoichiometry through hydrogen bonding, as shown by ¹H NMR studies. The data revealed that the substituents (Ph, *n*-Pr, and *t*-Bu) on the urea moiety strongly influence the binding ability of the receptors. ¹H NMR, UV–vis, and DFT studies showed that, in general, the association constants decreased with decreasing of anion basicity. Ph-urea 5a is the best anion receptor, showing the strongest affinity for F⁻ (log $K_{\text{assoc}} = 3.10$ and 4.6 in CDCl₃ and MeCN, respectively) and a complexation energy double of the next more stable complex. High complexation was also obtained for the oxoanions AcO⁻ and BzO⁻ with 5a. *t*-Bu-urea 5c was the weakest receptor, probably due to steric hindrance caused by the bulky *tert*-butyl groups. The binding results obtained followed the same trend by both techniques and were corroborated by DFT methods.

EXPERIMENTAL SECTION

Synthesis. All chemicals were reagent grade and were used without further purification. Chromatographic separations were performed on silica gel 60 (particle size 40–63 μm, 230–400 mesh). Melting points were measured (not corrected) and FTIR spectra were recorded. ¹H and ¹³C NMR spectra were recorded using a 500 MHz spectrometer, with TMS as internal reference. The conventional COSY 45 and the phase-sensitive NOESY experiments were collected as 256 × 2 K complex points. Elemental analysis was determined on a micro-analyser.

7,13,19,25-Tetra-*tert*-butyl-27,29-bis[(cyanopropyl)oxy]-28,30-dihydroxy-2,3-dihomo-3-oxacalix[4]arene (2). A mixture of *p*-*tert*-butyldihomooxalix[4]arene (6.0 g, 8.85 mmol), K₂CO₃ (2.45 g, 17.7 mmol), and 4-bromobutyronitrile (1.81 mL, 17.7 mmol) in CH₃CN (140 mL) was refluxed and stirred under N₂ for 6 days. After cooling, the solvent was evaporated under reduced pressure and the residue was dissolved in CH₂Cl₂ (250 mL) and washed with 1 M HCl (150 mL), H₂O (2 × 100 mL), and brine (2 × 100 mL). The organic layer was dried over Na₂SO₄ and filtered, and the solvent was removed under reduced pressure. The crude product was subjected to flash chromatography on silica gel (eluent CH₂Cl₂/MeOH, 99.5:0.5) affording a white solid in 49% yield (3.5 g). An analytically pure sample was obtained from recrystallization from MeOH: mp 175–177 °C; IR (KBr) 2247 cm⁻¹ (CN); ¹H NMR (CDCl₃, 500 MHz) δ 1.10, 1.23, 1.25, 1.27 [4s, 36H, C(CH₃)₃], 2.35–2.43 (m, 4H, OCH₂CH₂CH₂CN), 2.83–2.99 (m, 3H, OCH₂CH₂CH₂CN), 3.15–3.21 (m, 1H, OCH₂CH₂CH₂CN), 3.34, 4.42 (ABq, 2H, $J = 13.1$ Hz,

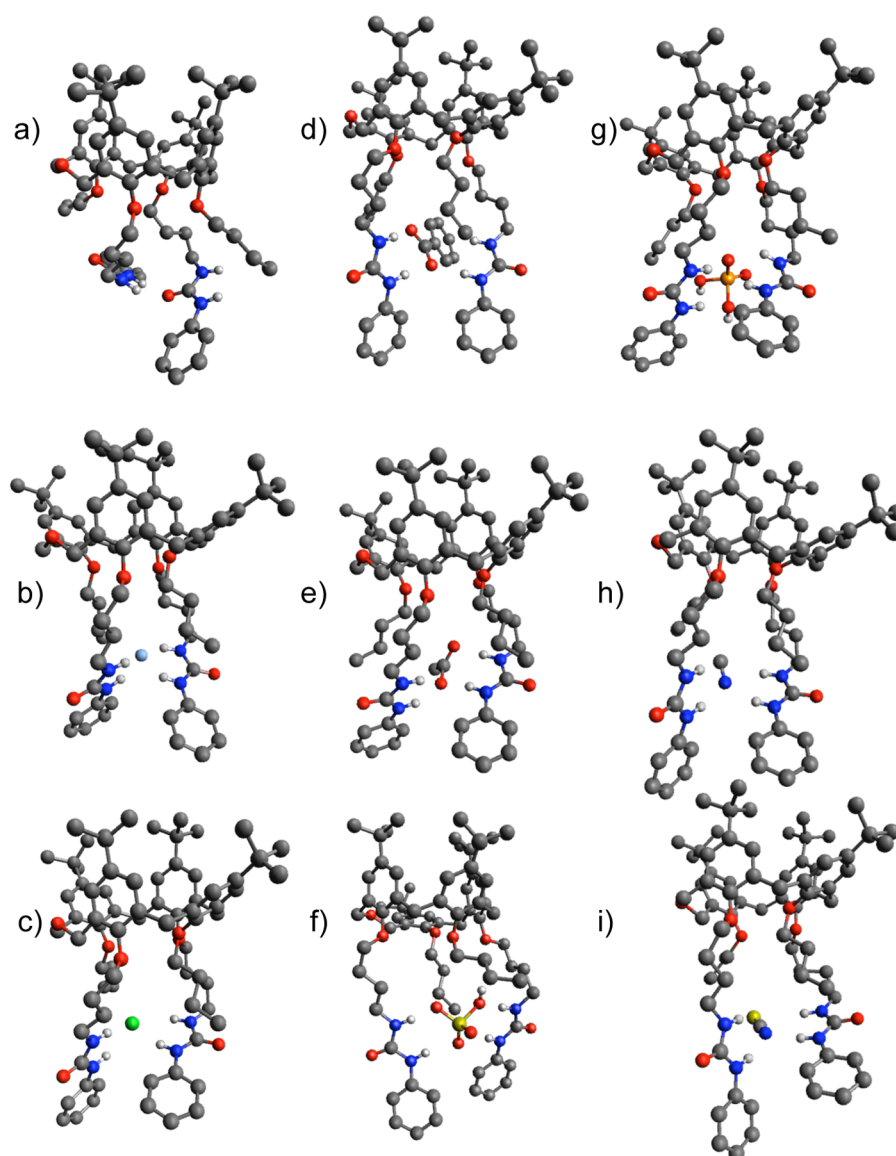


Figure 6. Optimized structures for Ph-urea **5a-X⁻** complexes: (a) **5a**, (b) **5a** + F⁻ (c) **5a** + Cl⁻, (d) **5a** + BzO⁻, (e) **5a** + AcO⁻, (f) **5a** + HSO₄⁻, (g) **5a** + H₂PO₄⁻, (h) **5a** + CN⁻ and (i) **5a** + SCN⁻. All of the hydrogen atoms were removed for clarity, except the urea NH hydrogens.

Table 5. Selected Structural Data of 5a-X⁻ Complexes (B3LYP/3-21G)

	NH...X ⁻ (Å)			
	a ₁	b ₁	a ₂	b ₂
5a-F⁻	1.69	1.68	1.78	1.61
5a-Cl⁻	2.35	2.32	2.40	2.28
5a-AcO⁻	1.73	1.92	1.77	1.82
5a-BzO⁻	1.85	1.81	2.96	1.88
5a-HSO₄⁻	1.78	1.96	1.74	2.19
5a-H₂PO₄⁻	1.87	1.85	1.89	2.37
5a-CN⁻	1.89	2.38	1.89	2.37
5a-SCN⁻	1.92	2.25	1.97	2.62

1 and 2 refer to the two ureido groups of **5a**.

ArCH₂Ar), 3.35, 4.54 (ABq, 2H, *J* = 12.8 Hz, ArCH₂Ar), 3.53, 4.10 (ABq, 2H, *J* = 13.3 Hz, ArCH₂Ar), 4.02–4.23 (3m, 4H, OCH₂CH₂CH₂CN), 4.25, 4.77 (ABq, 2H, *J* = 9.7 Hz, CH₂OCH₂), 4.43, 4.69 (ABq, 2H, *J* = 10.0 Hz, CH₂OCH₂), 6.88, 6.91, 7.01, 7.05, 7.06, 7.18, 7.28, 7.51 (8d, 8H, ArH), 7.12, 7.78 (2s, 2H, OH); ¹³C

NMR (CDCl₃, 125.8 MHz) δ 14.4, 14.5 (OCH₂CH₂CH₂CN), 26.2, 26.7 (OCH₂CH₂CH₂CN), 29.3, 30.0, 32.7 (ArCH₂Ar), 31.1, 31.4, 31.5, 31.6 [C(CH₃)], 33.9 (2C), 34.2, 34.3 [C(CH₃)], 71.5, 72.4 (CH₂OCH₂), 72.8, 73.7 (OCH₂CH₂CH₂CN), 119.1, 120.1 (CN), 123.9, 125.1, 125.4, 125.6, 126.0, 126.2, 128.0, 129.6 (ArH), 122.3, 127.2, 127.4, 128.4, 129.1, 131.9, 132.2, 135.1, 141.9, 142.4, 147.2, 147.6, 149.3 (2C), 152.5, 153.3 (Ar). Anal. Calcd for C₅₃H₆₈N₂O₅·MeOH: C, 76.75; H, 8.59; N, 3.32. Found: C, 77.07; H, 8.51; N, 3.57.

7,13,19,25-Tetra-tert-butyl-28,29-bis[(cyanopropyl)oxy]-27,30-dihydroxy-2,3-dihomo-3-oxacalix[4]arene (2a). From the previous flash chromatography, another set of fractions were combined and chromatographed again (eluent CH₂Cl₂/MeOH, 99.8:0.2) yielding **2a** in low yield: mp 143–145 °C; IR (KBr) 2250 cm⁻¹ (CN); ¹H NMR (CDCl₃, 500 MHz) δ 1.00, 1.26 [2s, 36H, C(CH₃)], 2.35 (m, 4H, OCH₂CH₂CH₂CN), 2.75, 2.87 (2m, 4H, OCH₂CH₂CH₂CN), 3.45, 4.20 (ABq, 4H, *J* = 13.9 Hz, ArCH₂Ar), 3.46, 4.45 (ABq, 2H, *J* = 13.5 Hz, ArCH₂Ar), 4.05, 4.23 (2m, 4H, OCH₂CH₂CH₂CN), 4.26, 4.67 (ABq, 4H, *J* = 10.0 Hz, CH₂OCH₂), 6.81, 6.86, 6.93, 7.23 (4d, 8H, ArH), 7.53 (s, 2H, OH); ¹³C NMR (CDCl₃, 125.8 MHz) δ 14.3 (OCH₂CH₂CH₂CN), 26.1 (OCH₂CH₂CH₂CN), 30.7, 31.6 (ArCH₂Ar), 31.0, 31.5 [C(CH₃)], 33.9, 34.0 [C(CH₃)], 71.6 (CH₂OCH₂), 72.8 (OCH₂CH₂CH₂CN), 119.7 (CN), 124.8, 125.1,

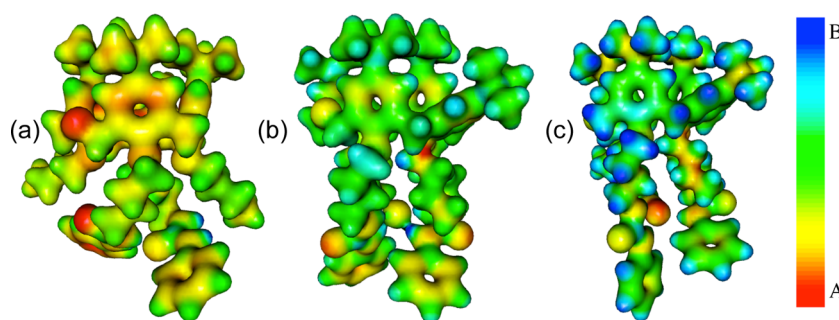


Figure 7. Electrostatic potential for Ph-urea **5a** and two anion complexes: (a) **5a**, (b) **5a** + F⁻ and (c) **5a** + SCN⁻. The electrostatic potential (in au) is represented over a constant electronic isodensity ρ (in \AA^{-3}) surfaces of volume V_s (in \AA^{-3}). All three figures correspond to $\rho = 0.05 \text{\AA}^{-3}$, and the potential varies: (a) from B = 0.33 (dark blue) to A = -0.17 (red) for the receptor; (b) from B = 0.13 (dark blue) to A = -0.31 (red) for the complex **5a-F⁻** and (c) from B = 0.07 (dark blue) to A = -0.37 (red) for the complex **5a-SCN⁻**.

126.1, 128.0 (ArH), 123.3, 128.0, 132.8, 133.3, 142.2, 147.0, 151.0, 151.7 (ArH). Anal. Calcd for $C_{53}H_{68}N_2O_5$: C, 78.29; H, 8.43; N, 3.45. Found: C, 78.54; H, 8.74; N, 3.61.

7,13,19,25-Tetra-tert-butyl-27,29-bis[(cyanopropyl)oxy]-28,30-dibutoxy-2,3-dihomo-3-oxacalix[4]arene (3). A mixture of **2** (1.0 g, 1.23 mmol) and 0.30 g (7.4 mmol) of NaH (60% oil dispersion) in 40 mL of THF–DMF (7:1, v/v) was stirred under an atmosphere of N₂. After 1 h, 0.85 mL (7.4 mmol) of 1-iodobutane was added, and the mixture was refluxed and stirred for 14 h. After cooling, the solvent was evaporated, and the residue was dissolved in CH₂Cl₂ (75 mL) and washed with 1 M HCl (2 × 40 mL), NH₄Cl saturated solution (3 × 30 mL), and brine (40 mL). The organic layer was dried over Na₂SO₄ and filtered, and the solvent was removed under reduced pressure. The crude product was subjected to flash chromatography on silica gel (eluent gradient from *n*-heptane/ethyl acetate 95:5 to 90:10) to give **3** as a white solid in the cone (0.55 g, 54% yield) and partial cone A conformations (0.14 g, 14% yield).

Cone: mp 104–106 °C; IR (KBr) 2247 cm⁻¹ (CN); ¹H NMR (CDCl₃, 500 MHz) δ 0.65, 1.04, 1.23, 1.34 [4s, 36H, C(CH₃)], 1.01, 1.03 (2t, 6H, *J* = 7.4 Hz, CH₃), 1.47, 1.55 (2m, 4H, OCH₂CH₂CH₂CH₃), 1.84 (m, 4H, OCH₂CH₂CH₂CH₃), 2.16, 2.28, 2.37, (3m, 4H, OCH₂CH₂CH₂CN), 2.60, 2.66 (2m, 4H, OCH₂CH₂CH₂CN), 3.22, 4.30 (ABq, 2H, *J* = 13.9 Hz, ArCH₂Ar), 3.23, 4.34 (ABq, 2H, *J* = 12.9 Hz, ArCH₂Ar), 3.26, 4.32 (ABq, 2H, *J* = 13.0 Hz, ArCH₂Ar), 3.59, 3.74, 3.85, 4.02 (4m, 8H, OCH₂CH₂CH₂CH₃ and OCH₂CH₂CH₂CN), 4.33, 4.65 (ABq, 2H, *J* = 13.2 Hz, CH₂OCH₂), 4.65, 4.77 (ABq, 2H, *J* = 13.0 Hz, CH₂OCH₂), 6.28, 6.79, 6.85, 6.89, 7.10, 7.12, 7.20, 7.22 (8d, 8H, ArH); ¹³C NMR (CDCl₃, 125.8 MHz) δ 14.0 (2C) [O(CH₂)₃CH₃], 14.1, 14.4, 19.3, 19.5 (OCH₂CH₂CH₂CN and OCH₂CH₂CH₂CH₃), 26.1, 26.3 (OCH₂CH₂CH₂CN), 29.7, 30.1, 30.5 (ArCH₂Ar), 31.2 (2C), 31.5, 31.6 [C(CH₃)], 32.4, 32.5 (OCH₂CH₂CH₂CH₃), 33.8, 33.9, 34.2, 34.3 [C(CH₃)], 67.7, 68.2 (CH₂OCH₂), 71.9 (2C), 74.8, 75.6 (OCH₂CH₂CH₂CN and OCH₂CH₂CH₂CH₃), 119.7, 120.3 (CN), 123.2, 124.3, 124.6, 125.1, 125.4, 126.5, 126.6, 127.0 (ArH), 130.0, 131.9, 132.3, 132.4, 132.6, 133.7, 133.9, 135.2, 144.8, 145.3, 145.8, 145.9, 151.3, 151.9, 152.0, 152.9 (Ar). Anal. Calcd for $C_{61}H_{84}N_2O_5$: C, 79.18; H, 9.15; N, 3.03. Found: C, 78.92; H, 9.12; N, 3.21.

Partial cone A: mp 108–110 °C; IR (KBr) 2243 cm⁻¹ (CN); ¹H NMR (CDCl₃, 500 MHz) δ 0.73 (m, 4H, OCH₂CH₂CH₂CN inverted), 0.96, 0.97 (2t, 6H, *J* = 7.4 Hz, CH₃), 1.21, 1.25, 1.38, 1.39 [4s, 36H, C(CH₃)], 1.38 (m, 4H, OCH₂CH₂CH₂CH₃), 1.66, 1.75, 1.92, 2.37 (4m, 10H, OCH₂CH₂CH₂CH₃, OCH₂CH₂CH₂CN and OCH₂CH₂CH₂CN inverted), 3.30, 4.39 (ABq, 2H, *J* = 13.1 Hz, ArCH₂Ar), 3.31, 4.28 (ABq, 2H, *J* = 13.1 Hz, ArCH₂Ar), 3.49–3.77 (several m, 6H, OCH₂CH₂CH₂CH₃ and OCH₂CH₂CH₂CN), 3.81, 3.88 (ABq, 2H, *J* = 15.8 Hz, ArCH₂Ar), 4.10, 5.05 (ABq, 2H, *J* = 11.9 Hz, CH₂OCH₂), 4.11 (s, 2H, CH₂OCH₂), 7.03, 7.05, 7.16, 7.22, 7.24, 7.32, 7.33 (7d, 8H, ArH); ¹³C NMR (CDCl₃, 125.8 MHz) δ 12.2, 13.2 (OCH₂CH₂CH₂CN inverted and OCH₂CH₂CH₂CN), 14.0 (2C) [O(CH₂)₃CH₃], 19.2, 19.3 (OCH₂CH₂CH₂CH₃), 25.2, 26.1 (OCH₂CH₂CH₂CN inverted and OCH₂CH₂CH₂CN), 29.1, 30.1,

39.2 (ArCH₂Ar), 31.4, 31.5, 31.6 (2C) [C(CH₃)], 32.1, 32.2 (OCH₂CH₂CH₂CH₃), 34.1 (2C), 34.2, 34.3 [C(CH₃)], 64.6, 68.5 (CH₂OCH₂), 70.3, 70.4, 73.9, 75.4 (OCH₂CH₂CH₂CN and OCH₂CH₂CH₂CH₃), 119.7, 121.1 (CN), 125.3, 125.9, 126.2, 126.7, 126.8, 126.9, 127.0, 128.2 (ArH), 130.2, 130.6, 132.9, 133.2, 133.4, 133.44, 134.5, 143.53, 145.3, 145.4, 145.8, 146.6, 152.4, 152.9, 153.7, 154.3 (Ar). Anal. Calcd for $C_{61}H_{84}N_2O_5$: C, 79.18; H, 9.15; N, 3.03. Found: C, 78.79; H, 9.06; N, 3.21.

7,13,19,25-Tetra-tert-butyl-27,29-bis[(aminobutyl)oxy]-28,30-dibutoxy-2,3-dihomo-3-oxacalix[4]arene (4). To a suspension of 1.0 g (1.08 mmol) of **3** (cone conformation) and 1.54 g (6.48 mmol) of CoCl₂·6H₂O in MeOH (35 mL) was slowly added 0.85 g (21.6 mmol) of NaBH₄. A black suspension was formed that was stirred at room temperature for 24 h. Then, another portion of NaBH₄ (0.85 g) was added, and the suspension was stirred for an additional 24 h. A 25% ammonia solution (110 mL) was added, and the mixture was stirred overnight. The solution was extracted with CH₂Cl₂ (3 × 50 mL) and dried over Na₂SO₄, and the solvent evaporated to dryness to afford diamine **4** as a beige solid (88% yield), which was pure enough to be immediately used in the next step: ¹H NMR (CDCl₃, 500 MHz) δ 0.90, 0.99, 1.16, 1.20 [4s, 36H, C(CH₃)], 1.00, 1.01 (2t, 6H, *J* = 7.4 Hz, CH₃), 1.42–1.67, 1.77–2.05 (several m, 16H, OCH₂CH₂CH₂CH₃ and OCH₂CH₂CH₂CH₂NH₂), 2.79 (2t, 4H, OCH₂CH₂CH₂CH₂NH₂), 3.18, 4.38 (ABq, 2H, *J* = 13.2 Hz, ArCH₂Ar), 3.18, 4.40 (ABq, 2H, *J* = 13.2 Hz, ArCH₂Ar), 3.22, 4.39 (ABq, 2H, *J* = 13.0 Hz, ArCH₂Ar), 3.61–3.90 (several m, 8H, OCH₂CH₂CH₂CH₃ and OCH₂CH₂CH₂CH₂NH₂), 4.59, 4.64 (ABq, 2H, *J* = 13.1 Hz, CH₂OCH₂), 4.59, 4.68 (ABq, 2H, *J* = 13.1 Hz, CH₂OCH₂), 6.62, 6.81, 6.93, 6.94, 6.97, 7.00, 7.03, 7.07 (8d, 8H, ArH).

Procedure for the Synthesis of Ureas 5a, 5b, and 5c. To a solution of **4** (0.90 g, 0.966 mmol) in CHCl₃ (30 mL) was added 1.93 mmol of the appropriate isocyanate. The mixture was stirred at room temperature under N₂ for 4 h. Evaporation of the solvent yielded the crude products which were purified as described below.

7,13,19,25-Tetra-tert-butyl-27,29-bis[(*N'*-phenylureido)butyl]oxy]-28,30-dibutoxy-2,3-dihomo-3-oxacalix[4]arene (5a). Flash chromatography (SiO₂, eluent CH₂Cl₂/MeOH, from 99:1 to 97:3) was followed by recrystallization from MeOH: 45% yield (0.56 g); mp 214–216 °C; IR (KBr) 3327 cm⁻¹ (NH), 1647 cm⁻¹ (CO); ¹H NMR (CDCl₃, 500 MHz) δ 0.55, 1.08, 1.33, 1.37 [4s, 36H, C(CH₃)], 0.91, 0.94 (2t, 6H, *J* = 7.4 Hz, CH₃), 1.44 (m, 4H, OCH₂CH₂CH₂CH₃), 1.50, 1.78, 1.92, 2.27 (4m, 12H, OCH₂CH₂CH₂CH₂NH_a and OCH₂CH₂CH₂CH₂CH₃), 3.20, 4.31 (ABq, 2H, *J* = 14.1 Hz, ArCH₂Ar), 3.21, 4.30 (ABq, 2H, *J* = 12.7 Hz, ArCH₂Ar), 3.22, 4.38 (ABq, 2H, *J* = 12.6 Hz, ArCH₂Ar), 3.21, 3.35, 3.55 (3m, 4H, OCH₂CH₂CH₂CH₂NH_a), 3.47, 3.58–3.81, 3.90, 3.99 (several m, 8H, OCH₂CH₂CH₂CH₃ and OCH₂CH₂CH₂CH₃), 4.39, 4.91 (ABq, 2H, *J* = 13.2 Hz, CH₂OCH₂), 4.40, 5.15 (ABq, 2H, *J* = 12.6 Hz, CH₂OCH₂), 5.82, 6.27 (2t, 2H, NH_a), 6.13, 6.47, 6.76, 6.94, 7.12, 7.20, 7.30, 7.31 (8d, 8H, ArH), 6.96, 7.01 (2t, 2H, Ph-H_a), 7.25, 7.27 (2t, 4H, Ph-H_m), 7.46, 7.4 (2d, 4H, Ph-H_o), 7.96, 8.05 (2s, 2H, NH_b); ¹³C

NMR (CDCl₃, 125.8 MHz) δ 13.9, 14.1 [O(CH₂)₃CH₃], 19.3, 19.4 (OCH₂CH₂CH₂CH₂CH₃), 25.4, 26.0, 26.2, 28.6 (OCH₂CH₂CH₂CH₂NH_a), 29.2, 30.9, 31.2 (ArCH₂Ar), 31.2, 31.3, 31.6, 31.7 [C(CH₃)], 32.2, 32.6 (OCH₂CH₂CH₂CH₃), 33.7, 33.9, 34.19, 34.21 [C(CH₃)], 39.6 (2C) (OCH₂CH₂CH₂CH₂NH_a), 70.8, 71.7 (CH₂OCH₂), 72.3, 74.7, 75.0, 75.5 (OCH₂CH₂CH₂CH₂NH_a and OCH₂CH₂CH₂CH₃), 118.9, 119.2, 121.8, 122.7, 123.8, 124.8, 125.0, 125.2, 125.9, 126.2, 126.9, 128.5, 128.8, 129.2 (ArH), 129.1, 131.0, 132.0, 132.7, 132.9, 134.37, 134.43, 136.0, 139.6, 140.1, 144.3, 145.0 (2C), 145.5, 152.6, 153.0, 153.9, 154.5 (Ar), 156.2, 156.9 (CO). Anal. Calcd for C₇₅H₉₈N₄O₇: C, 77.15; H, 8.46; N, 4.80. Found: C, 77.15; H, 8.69; N, 4.79.

7,13,19,25-Tetra-tert-butyl-27,29-bis[(n-propylureido)butyl]oxy]-28,30-dibutoxy-2,3-dihomo-3-oxacalix[4]arene (5b). Flash chromatography (SiO₂, eluent CH₂Cl₂/MeOH, from 99:1 to 96:4) was followed by recrystallization from CH₂Cl₂/*n*-hexane: 36% yield (0.42 g); mp 183–185 °C; IR (KBr) 3345 cm⁻¹ (NH), 1634 cm⁻¹ (CO); ¹H NMR (CDCl₃, 500 MHz) δ 0.55, 1.06, 1.29, 1.36 [4s, 36H, C(CH₃)], 0.95, 0.96, 0.97, 0.99 [4t, 12H, J = 7.3 Hz, O(CH₂)₃CH₃ and NH_bCH₂CH₂CH₃], 1.43–1.61, 1.68 (several m, 10H, OCH₂CH₂CH₂CH₃, NH_bCH₂CH₂CH₃ and OCH₂CH₂CH₂CH₂NH_a), 1.72–1.86, 1.91, 2.16 (3m, 10H, OCH₂CH₂CH₂CH₂NH_a and OCH₂CH₂CH₂CH₃), 3.19, 4.31 (ABq, 2H, J = 13.9 Hz, ArCH₂Ar), 3.20, 4.33 (ABq, 2H, J = 12.9 Hz, ArCH₂Ar), 3.21, 4.36 (ABq, 2H, J = 12.6 Hz, ArCH₂Ar), 3.14–3.35, 3.42 (several m, 8H, NH_bCH₂CH₂CH₃ and OCH₂CH₂CH₂CH₂NH_a), 3.49, 3.59–3.70, 3.75, 3.84, 3.91 (several m, 8H, OCH₂CH₂CH₂CH₂NH_a and OCH₂CH₂CH₂CH₃), 4.46, 4.59 (ABq, 2H, J = 13.4 Hz, CH₂OCH₂), 4.50, 4.92 (ABq, 2H, J = 12.9 Hz, CH₂OCH₂), 5.36, 5.59 (2t, 2H, NH_b), 5.51, 5.62 (2t, 2H, NH_a), 6.14, 6.65, 6.76, 6.88, 7.11, 7.20, 7.21, 7.25 (8d, 8H, ArH); ¹³C NMR (CDCl₃, 125.8 MHz) δ 11.5 (2C) (NH_bCH₂CH₂CH₃), 14.0, 14.1 [O(CH₂)₃CH₃], 19.3, 19.4 (OCH₂CH₂CH₂CH₃), 23.7 (2C) (NH_bCH₂CH₂CH₃), 25.9, 26.4, 26.6, 28.4 (OCH₂CH₂CH₂CH₂NH_a), 29.4, 30.8, 30.9 (ArCH₂Ar), 31.2, 31.3, 31.6, 31.7 [C(CH₃)], 32.2, 32.6 (OCH₂CH₂CH₂CH₃), 33.7, 33.9, 34.1, 34.2 [C(CH₃)], 39.8, 40.0, 41.9, 42.2 (OCH₂CH₂CH₂CH₂NH_a and NH_bCH₂CH₂CH₃), 69.5 (2C) (CH₂OCH₂), 72.6, 74.4, 74.9, 75.4 (OCH₂CH₂CH₂CH₂NH_a and OCH₂CH₂CH₂CH₃), 123.6, 124.0, 124.5, 125.0, 125.6, 126.3, 126.9, 127.4 (ArH), 129.3, 131.6, 132.2, 132.66, 132.70, 134.2 (2C), 135.9, 144.3, 145.0, 145.1, 145.3, 152.5, 152.6, 153.3, 153.8 (Ar), 159.1, 159.2 (CO). Anal. Calcd for C₆₉H₁₀₂N₄O₇: C, 75.37; H, 9.35; N, 5.10. Found: C, 75.02; H, 9.29; N, 5.20.

7,13,19,25-Tetra-tert-butyl-27,29-bis[(tert-butylureido)butyl]oxy]-28,30-dibutoxy-2,3-dihomo-3-oxacalix[4]arene (5c). Flash chromatography (SiO₂, eluent CH₂Cl₂/MeOH, from 99:1 to 95:5): 49% yield (0.59 g); mp 160–162 °C; IR (KBr) 3366 cm⁻¹ (NH), 1638 cm⁻¹ (CO); ¹H NMR (CDCl₃, 500 MHz) δ 0.54, 1.07, 1.30, 1.36 [4s, 36H, C(CH₃)], 0.96, 0.98 [2t, 6H, J = 7.5 Hz, O(CH₂)₃CH₃], 1.38, 1.43 [2s, 18H, NH_bC(CH₃)], 1.41–1.52 (m, 6H, OCH₂CH₂CH₂CH₃ and OCH₂CH₂CH₂CH₂NH_a), 1.64–1.93, 2.19 (several m, 10H, OCH₂CH₂CH₂CH₃ and OCH₂CH₂CH₂CH₂NH_a), 3.19, 4.36 (ABq, 2H, J = 12.6 Hz, ArCH₂Ar), 3.20, 4.31 (ABq, 2H, J = 12.6 Hz, ArCH₂Ar), 3.21, 4.29 (ABq, 2H, J = 13.5 Hz, ArCH₂Ar), 3.18–3.27, 3.48 (several m, 4H, OCH₂CH₂CH₂CH₂NH_a), 3.36, 3.57–3.80, 3.87–3.98 (several m, 8H, OCH₂CH₂CH₂CH₂NH_a and OCH₂CH₂CH₂CH₃), 4.46, 4.67 (ABq, 2H, J = 13.3 Hz, CH₂OCH₂), 4.47, 4.95 (ABq, 2H, J = 12.6 Hz, CH₂OCH₂), 5.16, 5.58 (2s, 2H, NH_b), 5.56, 5.57 (2t, 2H, NH_a), 6.12, 6.62, 6.76, 6.90, 7.11, 7.20, 7.22, 7.25 (8d, 8H, ArH); ¹³C NMR (CDCl₃, 125.8 MHz) δ 14.0, 14.1 [O(CH₂)₃CH₃], 19.3, 19.4 (OCH₂CH₂CH₂CH₃), 25.5, 26.4, 26.5, 28.5 (OCH₂CH₂CH₂CH₂NH_a), 29.6, 30.8, 31.1 (ArCH₂Ar), 29.7, 29.8 [NH_bC(CH₃)], 31.2, 31.3, 31.6, 31.7 [C(CH₃)], 32.3, 32.7 (OCH₂CH₂CH₂CH₃), 33.7, 33.9, 34.1, 34.2 [C(CH₃)], 39.3, 39.5 (OCH₂CH₂CH₂CH₂NH_a), 49.9, 50.2 [NH_bC(CH₃)], 69.6, 69.9 (CH₂OCH₂), 72.4, 74.8, 74.9, 75.4 (OCH₂CH₂CH₂CH₂NH_a and OCH₂CH₂CH₂CH₃), 123.6, 124.0, 124.5, 125.1, 125.6, 126.2, 126.9, 127.6 (ArH), 129.1, 131.5, 132.2, 132.7, 132.8, 134.1, 134.3, 136.0, 144.3, 144.9, 145.1, 145.4, 152.6, 152.7, 153.6, 153.9 (Ar), 158.4 (2C)

(CO). Anal. Calcd for C₇₁H₁₀₆N₄O₇: C, 75.63; H, 9.47; N, 4.97. Found: C, 75.60; H, 9.30; N, 5.03.

¹H NMR Titrations. The association constants (as log K_{assoc}) were determined in CDCl₃ by ¹H NMR titration experiments. Several aliquots (up to 10 equiv) of the anion solutions (as tetrabutylammonium salts) were added to 0.5 mL solution of the receptors (2.5×10^{-3} – 5×10^{-3} M) directly in the NMR tube. The spectra were recorded after each addition of the salts, and the temperature of the NMR probe was kept constant at 25 °C. For each anion–receptor system titrations were repeated at least two times. The association constants were evaluated using the WinEQNMR2 program²³ and following the urea NH chemical shifts. When possible, K_{assoc} was calculated as a mean value of the four NH chemical shifts. The Job methods were performed keeping the total concentration in the same range as before.

UV–vis Titrations. The association constants were also determined in acetonitrile by absorption spectrophotometry at 25.0 ± 0.1 °C. The spectra were recorded between 260 and 310 nm, using quartz cells with an optical path length of 1 cm. The anions studied were provided as tetrabutylammonium salts, and were dried under vacuum for at least 24 h before use. Twenty additions of 10 μ L of the anion solution were directly added into the cell containing 2 mL of the receptor solution (C_{r} from 10^{-5} to 2×10^{-4} M). The anion to receptor ratios were in the range 1–10. The spectral changes were interpreted using the SPECFIT program.³²

Theoretical Methods. Computational density functional theory (DFT) methods were used to analyze the structure and electronic properties of all the conformers studied. All the structures were fully optimized without symmetry constraints using the Becke three-parameter hybrid functional combined with the Lee, Yang, and Parr correlation functional (B3LYP)³⁰ along with the split-valence double- ζ Pople basis set, which is well-known to produce accurate geometries. Following this optimization, a single-point energy calculation with the same functional and a bigger basis was made, using 6-31G(d,p) valence double- ζ polarized basis set.

The methods and basis sets used were those implemented in the Gaussian 03 software package.³³ The vibrational frequency calculations were performed at the same level of theory to check that all structures were at the global minima of the potential energy surface (denoted by an absence of negative vibrational frequencies) and to correct the computed energies for zero-point energies as well as translational, rotational and vibrational contributions to the enthalpy. All the figures and electrostatic potential surfaces were constructed using Molekel software.³⁴

The electrostatic potential was drawn over a surface of constant electronic isodensity using Molekel software. All the data needed to generate these surfaces and electrostatic potentials were calculated with Gaussian 03 software.

For each anion several initial positions were tested, starting inside or outside the receptor cavity. The relative complexation energies (ΔE_{c} corresponding to the process $5\text{a} + \text{X}^- \rightarrow [5\text{a} - \text{X}^-]$, where X^- represents each one of the anions) were calculated as the energy difference at 298 K between the final energy of the complexes and the sum of the energies of 5a and the anion in study, at the same theoretical level.³⁵

■ ASSOCIATED CONTENT

📄 Supporting Information

¹H and ¹³C NMR spectra of the new compounds **2**, **2a**, **3** (cone), **3** (cone partial), **5a**, **5b**, and **5c**, and 2D NOESY spectra of compounds **2a** and **3** (partial cone). Table of atom coordinates and absolute energies. This material is available free of charge via the Internet at <http://pubs.acs.org>.

■ AUTHOR INFORMATION

Corresponding Author

*E-mail: pmmarcos@fc.ul.pt.

Notes

The authors declare no competing financial interest.

ACKNOWLEDGMENTS

We thank the Fundação para a Ciência e a Tecnologia, Project ref PTDC/QUI/69858/2006.

REFERENCES

- (1) (a) Arnaud-Neu, F.; McKervey, M. A.; Schwing-Weill, M. J. In *Calixarenes 2001*; Asfari, Z., Böhmer, V., Harrowfield, J., Vicens, J., Eds.; Kluwer Academic: Dordrecht, 2001; pp 385–406. (b) Roundhill, D. M.; Shen, J. Y. In *Calixarenes 2001*; Asfari, Z., Böhmer, V., Harrowfield, J., Vicens, J., Eds.; Kluwer Academic: Dordrecht, 2001; pp 407–420. (c) Arnaud-Neu, F.; Schwing-Weill, M. J.; Dozol, J.-F. In *Calixarenes 2001*; Asfari, Z., Böhmer, V., Harrowfield, J., Vicens, J., Eds.; Kluwer Academic: Dordrecht, 2001; pp 642–662.
- (2) Matthews, S. E.; Beer, P. D. *Supramol. Chem.* **2005**, *17*, 411–435.
- (3) Ai-Fang, L.; Wang, J.-H.; Wang, F.; Jiang, Y.-B. *Chem. Soc. Rev.* **2010**, *39*, 3729–3745.
- (4) Gale, P. A. *Chem. Soc. Rev.* **2010**, *39*, 3746–3771.
- (5) Amendola, V.; Fabbrizzi, L.; Mosca, L. *Chem. Soc. Rev.* **2010**, *39*, 3889–3915.
- (6) Edwards, N. Y.; Possanza, A. L. *Supramol. Chem.* **2013**, *25*, 446–463.
- (7) Scheerder, J.; Fochi, M.; Engbersen, F. J.; Reinhoudt, D. N. *J. Org. Chem.* **1994**, *59*, 7815–7820.
- (8) Kang, S. O.; Oh, J. M.; Yang, Y. S.; Chun, J. C.; Jeon, S.; Nam, K. C. *Bull. Korean Chem. Soc.* **2002**, *23*, 145–148.
- (9) Schazmann, B.; Diamond, D. *New J. Chem.* **2007**, *31*, 587–592.
- (10) Babu, J. N.; Bhalla, V.; Kumar, M.; Puri, R. K. *New J. Chem.* **2009**, *33*, 675–681.
- (11) Modi, N. R.; Patel, B.; Patel, M. B.; Menon, S. K. *Talanta* **2011**, *86*, 121–127.
- (12) Stastny, V.; Lhotak, P.; Michlova, V.; Stibor, I.; Sykora, J. *Tetrahedron* **2002**, *58*, 7207–7211.
- (13) Stibor, I.; Budka, J.; Michlova, V.; Tkadlecova, M.; Pojarova, M.; Curinova, P.; Lhotak, P. *New J. Chem.* **2008**, *32*, 1597–1607.
- (14) Curinova, P.; Stibor, I.; Budka, J.; Sykora, J.; Kamil, L.; Lhotak, P. *New J. Chem.* **2009**, *33*, 612–619.
- (15) Capici, C.; De Zorzi, R.; Gargiulli, C.; Gattuso, G.; Geremia, S.; Notti, A.; Pappalardo, S.; Parisi, M. F.; Puntoriero, F. *Tetrahedron* **2010**, *66*, 4987–4993.
- (16) Scheerder, J.; Engbersen, F. J.; Casnati, A.; Ungaro, R.; Reinhoudt, D. N. *J. Org. Chem.* **1995**, *60*, 6448–6454.
- (17) Hamon, M.; Ménand, M.; Le Gac, S.; Luhmer, M.; Dalla, V.; Jabin, I. *J. Org. Chem.* **2008**, *73*, 7067–7071.
- (18) Masci, B. In *Calixarenes 2001*; Asfari, Z., Böhmer, V., Harrowfield, J., Vicens, J., Eds.; Kluwer Academic: Dordrecht, 2001; pp 235–249.
- (19) Marcos, P. M.; Proença, C. S.; Teixeira, F. A.; Ascenso, J. R.; Bernardino, R. J.; Cragg, P. J. *Tetrahedron* **2013**, *69*, 7430–7437.
- (20) Jaime, C.; de Mendoza, J.; Prados, P.; Nieto, P.; Sanchez, C. *J. Org. Chem.* **1991**, *56*, 3372–3376.
- (21) Marcos, P. M.; Ascenso, J. R.; Pereira, J. L. C. *Eur. J. Org. Chem.* **2002**, 3034–3041.
- (22) Marcos, P. M.; Ascenso, J. R.; Lamartine, R.; Pereira, J. L. C. *Tetrahedron* **1997**, *53*, 11791.
- (23) Hynes, M. J. *J. Chem. Soc., Dalton Trans.* **1993**, 311–312.
- (24) Izutsu, K. *Electrochemistry in Nonaqueous Solutions*; Wiley-VCH Verlag: Weinheim, 2002; pp 66–67.
- (25) Pérez-Casas, C.; Yatsimirsky, A. K. *J. Org. Chem.* **2008**, *73*, 2275–2284.
- (26) Goursaud, M.; De Bernardin, P.; Cort, A. D.; Bartik, K.; Bruylants, G. *Eur. J. Org. Chem.* **2012**, 3570–3574.
- (27) Boiocchi, M.; Del Boca, L.; Gómez, D. E.; Fabbrizzi, L.; Licchelli, M.; Monzani, E. *J. Am. Chem. Soc.* **2004**, *126*, 16507–16514.
- (28) Amendola, V.; Gómez, D. E.; Fabbrizzi, L.; Licchelli, M. *Acc. Chem. Res.* **2006**, *39*, 343–353.
- (29) (a) Trummal, A.; Rummel, A.; Lippmaa, E.; Koppel, I.; Koppel, I. A. *J. Phys. Chem. A* **2011**, *115*, 6641–6645. (b) Bos, M.; van der Linden, W. E. *Anal. Chim. Acta* **1996**, *332*, 201–211.
- (30) (a) Becke, A. D. *J. Chem. Phys.* **1993**, *98*, 5648–5652. (b) Becke, A. D. *Phys. Rev. A* **1998**, *38*, 3098–3100. (c) Lee, C.; Yang, W.; Parr, R. G. *Phys. Rev. B* **1988**, *37*, 785–789.
- (31) Hehre, W. J.; Radom, L.; Schleyer, P. R.; Pople, J. A. *Ab Initio Molecular Orbital Theory*; Wiley: New York, 1985.
- (32) Gampp, H.; Maeder, M.; Meyer, C. J.; Zueberbühler, A. D. *Talanta* **1985**, *32*, 257–264.
- (33) Frisch, M. J.; Trucks, G. W.; Schlegel, H. B.; Scuseria, G. E.; Robb, M. A.; Cheeseman, J. R.; Montgomery, J. A., Jr.; Vreven, T.; Kudin, K. N.; Burant, J. C.; Millam, J. M.; Iyengar, S. S.; Tomasi, J.; Barone, V.; Mennucci, B.; Cossi, M.; Scalmani, G.; Rega, N.; Petersson, G. A.; Nakatsuji, H.; Hada, M.; Ehara, M.; Toyota, K.; Fukuda, R.; Hasegawa, J.; Ishida, M.; Nakajima, T.; Honda, Y.; Kitao, O.; Nakai, H.; Klene, M.; Li, X.; Knox, J. E.; Hratchian, H. P.; Cross, J. B.; Bakken, V.; Adamo, C.; Jaramillo, J.; Gomperts, R.; Stratmann, R. E.; Yazyev, O.; Austin, A. J.; Cammi, R.; Pomelli, C.; Ochterski, J. W.; Ayala, P. Y.; Morokuma, K.; Voth, G. A.; Salvador, P.; Dannenberg, J. J.; Zakrzewski, V. G.; Dapprich, S.; Daniels, A. D.; Strain, M. C.; Farkas, O.; Malick, D. K.; Rabuck, A. D.; Raghavachari, K.; Foresman, J. B.; Ortiz, J. V.; Cui, Q.; Baboul, A. G.; Clifford, S.; Cioslowski, J.; Stefanov, B. B.; Liu, G.; Liashenko, A.; Piskorz, P.; Komaromi, I.; Martin, R. L.; Fox, D. J.; Keith, T.; Al-Laham, M. A.; Peng, C. Y.; Nanayakkara, A.; Challacombe, M.; Gill, P. M. W.; Johnson, B.; Chen, W.; Wong, M. W.; Gonzalez, C.; Pople, J. A. *Gaussian 03, Revision C.02*; Gaussian, Inc., Wallingford, CT, 2004.
- (34) Flükiger, P. *Molekel, Molecular Visualisation Software*; University of Geneva (<http://www.bioinformatics.org/molkel/wiki/>).
- (35) Bernardino, R. J.; Cabral, B. *Supramol. Chem.* **2002**, *14*, 57–66.